NASA TECHNICAL NOTE

NASA TN D-7354

NASA TN D-7354

SCATTERING OF 42-MeV ALPHA PARTICLES FROM COPPER-65

by William M. Stewart and Kamal K. Seth

Lewis Research Center

Cleveland, Ohio 44135

NATIONAL AERONAUTICS AND SPACE ADMINISTRATION • WASHINGTON, D. C. • JULY 1973

1. Report No.	2. Government Accession No.	3. Recipient's Catalog No.
NASA TN D-7354		

4. Title and Subtitle	5. Report Date
SCATTERING OF 42-MeV ALPHA PARTICLES FROM COPPER-65	July 1973
	6. Performing Organization Code

7. Author(s)	8. Performing Organization Report No.
William M. Stewart, Lewis Research Center; and Kamal K. Seth, Northwestern University, Evanston, Illinois	E-7404
	10. Work Unit No. 503-10
9. Performing Organization Name and Address	11. Contract or Grant No.
Lewis Research Center National Aeronautics and Space Administration Cleveland, Ohio 44135	
	13. Type of Report and Period Covered
12. Sponsoring Agency Name and Address	Technical Note
National Aeronautics and Space Administration Washington, D.C. 20546	14. Sponsoring Agency Code

15. Supplementary Notes

16. Abstract

42-MeV alpha particles have been elastically and inelastically scattered from ^{65}Cu in an attempt to excite states which may be described in terms of an excited core model. Angular distributions ($10^{o} \leq \theta_{cm} \leq 50^{o}$) were measured for 17 excited states. Seven of the excited states had angular distributions similar to a core quadrupole excitation and eight of the excited states had angular distributions similar to a core octupole excitation. The excited state at 2.858 MeV had an angular distribution which suggests that it may have resulted from the particle coupling to a two-phonon core state. An extended particle-core coupling calculation was performed and the predicted energy levels and reduced transition probabilities compared to the experimental data. The low-lying levels are described quite well and the wavefunctions of these states explain the large spectroscopic factors measured in stripping reactions. For ^{65}Cu the coupling of the particle to the core is no longer weak as in the simpler model, and configuration mixing results.

17. Key Words (Suggested by Author(s))

Nuclear reactions
Copper-65
Alpha scattering
Weak-coupling model
Nuclear spectroscopy
Nuclear energy levels
Transition probabilities

18. Distribution Statement

Unclassified - unlimited

19. Security Classif. (of this report)	20. Security Classif. (of this page)	21. No. of Pages	22. Price*
Unclassified	Unclassified	28	$3.00

* For sale by the National Technical Information Service, Springfield, Virginia 22151

SCATTERING OF 42-MeV ALPHA PARTICLES FROM COPPER-65

by William M. Stewart and Kamal K. Seth*

Lewis Research Center

SUMMARY

42-MeV alpha particles have been elastically and inelastically scattered from ^{65}Cu in an attempt to excite states which may be described in terms of an excited core model. Angular distributions ($10^{o} \leq \theta_{cm} \leq 50^{o}$) were measured for 17 excited states. Seven of the excited states had angular distributions similar to a core quadrupole excitation and eight of the excited states had angular distributions similar to a core octupole excitation. The excited state at 2.858 MeV had an angular distribution which suggests that it may have resulted from the particle coupling to a two-phonon core state. An extended particle-core coupling calculation was performed and the predicted energy levels and reduced transition probabilities compared to the experimental data. The low-lying levels are described quite well and the wavefunctions of these states explain the large spectroscopic factors measured in stripping reactions. For ^{65}Cu the coupling of the particle to the core is no longer weak as in the simpler model, and configuration mixing results.

INTRODUCTION

The description of odd A nucleus in terms of the weak-coupling model in the limit of zero coupling strength has had limited success (ref. 1). The ^{63}Cu and ^{65}Cu nuclei have been studied by inelastic scattering (refs. 2 to 5), and the experimental results do not agree with the zero-strength model. Also the collective property of the low-lying states has been questioned because of the large spectroscopic factors measured in stripping (ref. 6) and pickup (ref. 7) reactions for ^{63}Cu and ^{65}Cu. An extension of the zero-strength model by Thankappan and True (ref. 8) described the low-lying levels of ^{63}Cu quite well and explained the large spectroscopic factors by including more than one single particle orbit and allowing configuration mixing, by means of a finite coupling strength. Recent shell model calculations (ref. 9) for ^{63}Cu and ^{65}Cu have shown that

*Associate Professor of Physics, Northwestern University, Evanston, Illinois.

such an extended particle-core coupling scheme with configuration mixing is a good approximation to the more exact shell model calculations.

Scattering of 42-MeV alpha particles is known to excite collective states. This experiment was done with better energy resolution (ref. 5) and a higher bombarding energy (ref. 4) than previous alpha particle scattering experiments on ^{65}Cu. The extended particle-core model was used to calculate the energy levels and reduced transition probabilities for ^{65}Cu and the results are compared to the experimental values.

EXPERIMENTAL ARRANGEMENT

The experiment was done using the 42-MeV alpha particle beam of the NASA Lewis 160-centimeter cyclotron. A schematic drawing of the scattering system is shown in figure 1. The scattering system included magnetic analysis of the incident beam and particle detection by lithium-drifted silicon detectors (ref. 10). Complete details of the scattering system are given elsewhere (ref. 11). A four detector mount allowed simultaneous measurements of cross sections at four different angles. Data taken forward of 20° had a detector separation of 2° and an angular resolution of 0.06°. Beyond 20° the angular separation was increased to 4° and a resulting angular resolution of 0.12°. The accuracy of the angle setting was 0.05° and the zero direction was determined by right-left scattering. A block diagram of the electronics is shown in figure 2. The overall energy resolution of the experiment was 80 to 100 keV and angular distributions were measured from 10° to 50° in the center of mass system. This angular range was sufficient to establish the angular momentum involved in the transition.

Absolute Cross Sections

The target was an isotopically enriched foil (99.64 percent ^{65}Cu). The areal density of the target was determined by measuring the energy loss of an 8.78-MeV alpha particle in passing through the foil. The areal density of the foil was measured to be 0.694 milligram per square centimeter. The total error in the absolute cross section is estimated to be 10 percent, and the error in the relative cross sections is 3 percent. The cross sections are listed in table I, and the errors quoted in the table are the statistical uncertainties.

Energy Spectra-Reduction and Excitation Energies

A typical energy spectrum is shown in figure 3. The number of counts in the elastic and inelastic peaks was found by fitting the energy spectra with a skewed Gaussian func-

tion using a least-squares computer program (ref. 12) with a linear background search. The peak shape was determined by fitting the elastic peak and held fixed for fitting all the other peaks in the spectrum. The energy calibration for each of the four detectors was based on the known energies of the ground and first six excited states. The excitation energies measured in this experiment are accurate to ±25 keV. The angular momentum transfer of the reaction l was determined by comparing the shapes of the angular distributions to the calculated angular distribution. The partial deformation parameter $\beta_l'(J_f)$ was obtained for each inelastic angular distribution by normalizing the calculated cross sections to the experimental data. All the inelastic states that were excited strongly enough in the experiment to obtain angular distributions are listed in table III, along with the corresponding partial deformation parameter.

The partial deformation parameter is defined by

$$\left(\frac{d\sigma}{d\Omega}\right)_{J_f}^{exp} = \left[\beta_l'(J_f)\right]^2 \left(\frac{d\sigma}{d\Omega}\right)_{DWBA} \tag{1}$$

(Symbols are defined in the appendix.)

In the limit of weak particle-core coupling, the partial deformation parameter $\beta_l'(J_f)$ for the odd A nucleus is related to the deformation parameter $\beta_l(\text{core})$ of its neighboring even A core nucleus by

$$\beta_l'(J_f) = \left[\frac{2J_f + 1}{(2J_i + 1)(2l + 1)}\right]^{1/2} \beta_l(\text{core}) \tag{2}$$

where

J_f excited state spin of odd A nucleus

J_i ground state spin of odd A nucleus

l angular momentum transfer

If equation (2) is summed over all the allowed excited states, it follows that

$$\left[\beta_l(\text{core})\right]^2 = \sum_{J_f} \left[\beta_l'(J_f)\right]^2 \tag{3}$$

The collective nuclear model relates the nuclear deformation parameter to the reduced transition probability $B(El)\uparrow$ for electromagnetic excitation of a one-phonon state (ref. 14)

$$B(E\ell)\uparrow = \left(\frac{3}{4\pi}\right)^2 \left(ZeR_o^{\ell}\right)^2 \beta_{\ell}^2(\text{core}) \tag{4}$$

EXPERIMENTAL RESULTS AND ANALYSIS

The differential cross sections were measured for the elastic state and seventeen inelastic states. The experimentally measured distributions are shown in figures 4, 5, and 6. The elastic scattering data were fit by using the optical model with a six parameter Woods-Saxon potential given by

$$U(r) = V_c - V\left\{1 + \exp\left[\frac{r - r_o A^{1/3}}{a_o}\right]\right\}^{-1} - iW\left\{1 + \exp\left[\frac{r - r_i A^{1/3}}{a_i}\right]\right\}^{-1} \tag{5}$$

where

$U(r)$	scattering potential
V_c	Coulomb potential
V	strength of real term of nuclear optical potential
r_o	radius of real term of nuclear optical potential
a_o	diffuseness of real term of nuclear optical potential
W	strength of imaginary term of nuclear optical potential
r_i	radius of imaginary term of nuclear optical potential
a_i	diffuseness of imaginary term of nuclear optical potential

The computer program SCATLE (ref. 13) was used to do the calculation. The best fit calculation is shown in figure 4, and the resulting parameters are listed in table II.

The inelastic scattering angular distributions were compared with the predictions of a distorted wave Born approximation using the computer program DWUCK (information received from P. D. Kunz of Univ. of Colorado). A surface interaction was used in the form factor and complex coupling was included. Coulomb excitation was also included in the calculation. The best fit optical model potential was used to calculate the scattering waves and the collective model form factor. The particle-core model predicts that the electromagnetic transition probability $B(E\ell)$ to the ground state should be approximately equal to that for the collective core state. This implies that the cross section for inelastic scattering to any member of the multiplet should be proportional to $(2J_f + 1)$ and that

the total cross section for excitation of the multiplet should be equal to that for excitation of the collective core state. In addition the shape of the angular distribution for each member of the multiplet should resemble the angular distribution for the corresponding core state. The relative transition strengths of the excited states are measured by the partial deformation parameters $\beta'_l(J_f)$ and listed in table III. Using the spin assignments from previous works (ref. 15), the total deformation parameter β_l(core) can be calculated using equation (2). Since only the core is assumed to be excited, the reduced transition probabilities for ^{65}Cu relative to the ^{64}Ni core are found by taking the ratio of β_l^2(core)/$\beta_l^2(^{64}\text{Ni})$. These values of β_l(core) and the ratios of the reduced transition probabilities are listed in table III. The experimental value of the deformation parameter for ^{64}Ni was taken from reference 3. Also shown in table III are the ratios of the reduced transition probabilities measured for 17.5-MeV proton scattering (ref. 3) and 29-MeV alpha particle scattering (ref. 4).

The inelastic angular distributions of the excited states with angular momentum transfers of $l = 2$ are shown in figure 5 along with the corresponding DWBA calculations. The angular momentum transfers and the partial deformation parameters are assigned on the basis of the DWBA calculations. The zero-strength coupling model predicts four states with their transition strengths proportional to $(2J_f + 1)$ and with an energy centroid equal to the energy of the 2^+ core state of ^{64}Ni. Experimentally three strongly excited states and four weaker states with an $l = 2$ angular distribution are found. The excited state at 2.858-MeV has been assigned an $l = 3$ transfer by Kumabe, Matoba, and Takasaki (ref. 4). In this experiment at 42 MeV, the angular distribution is fit by an $l = 2$ DWBA calculation, although the large angle fit is not as good as the other $l = 2$ angular distributions. Since at 29 MeV (ref. 4) the 2.858-MeV state was in phase with the elastic angular distribution and at 42 MeV is out of phase with the elastic angular distribution, the energy dependence of the angular distribution of this state along with its relatively high excitation energy, suggest that it may result from the $p_{3/2}$ proton coupling to one of the two-phonon states in ^{64}Ni. The phase relation of the two-phonon angular distribution to that of the elastic angular distribution has been shown (refs. 16 and 17) to be energy dependent for the nickel isotopes.

Of the predicted quartet of states corresponding to the coupling of the $p_{3/2}$ proton to the 2^+ core state, only three states are excited with the expected strength. The $3/2^-$ state at 1.725 MeV is excited too weakly to fit the $(2J_f + 1)$ strength predicted by the simple model, although it gives an excellent energy centroid prediction. Perey (ref. 18) suggested that the strength of the $3/2^-$ state would be weakened due to mixing with the ground state. The zero-strength particle-core model has its greatest success if the ground state spin is not included in the spins of the excited multiplet (refs. 1 and 19).

There are seven states observed experimentally with an $l = 2$ angular distribution. If the total transition strength of the 2^+ core state of ^{64}Ni is considered mixed into

all seven of the $l = 2$ angular distributions, then from equation (3), $\beta_2(\text{core}) = 0.166 \pm 0.014$. If this is compared to the deformation for the ^{64}Ni core state, $\beta_2(^{64}\text{Ni}) = 0.200 \pm 0.015$, the agreement is reasonable. The total core strength is not observed experimentally which suggests that there are some weakly excited states that were not observed.

The inelastic angular distributions for the excited states observed with an angular momentum transfer of $l = 3$ are shown in figure 6 along with the corresponding DWBA calculations. Again on the basis of the weak-coupling model, four excited states are expected. Four strongly excited and four weaker excited states are observed all having an $l = 3$ angular distribution. The state at 3.930 MeV has not been observed in previous inelastic scattering experiments (refs. 3 to 5).

Little can be said about the octupole-coupled states because the spins of the resulting states of ^{65}Cu are unknown. The excited state at 2.530 MeV is the strongest excited state for an $l = 3$ transition, as was the case for the other inelastic scattering (refs. 3 and 4). Blair (ref. 6) reports a strong $l = 4$ transition to a state of 2.54 MeV. Also, Bachner, Bock, and Duhm (ref. 7) report the pickup reaction on ^{66}Zn to the 2.535-MeV state of ^{65}Cu is too strong to be explained by $g_{9/2}$ admixtures in the ^{66}Zn ground state, and therefore collective contributions must be responsible for the strong excitation of this state. If this is the state that is excited in the inelastic scattering experiments, there must be considerable configuration mixing.

Again if it assumed that the core octupole transition strength is spread over all eight of the $l = 3$ angular distributions, then $\beta_3(\text{core}) = 0.150 \pm 0.011$ as compared to $\beta_3(^{64}\text{Ni}) = 0.181 \pm 0.016$ for the 3^- state of ^{64}Ni. The agreement is not as good as for the $l = 2$ transitions, but again the total core strength is not observed.

PARTICLE-CORE COUPLING CALCULATION

A recent shell model calculation (ref. 9) with a realistic effective force in the $1f_{5/2}$, $2p_{3/2}$, $2p_{1/2}$ orbitals performed for ^{65}Cu has shown that an extended particle-core coupling scheme with finite coupling strength and configuration mixing gives a good approximation to the more exact calculation. Thankappan and True (ref. 8) did a calculation of this type for ^{63}Cu. On the basis of the experimental evidence that the collective- and single-particle states are mixed for ^{65}Cu, the calculation was extended to ^{65}Cu.

The coupling between the particle and the core is a scalar which can be written as a sum of scalar products of a tensor of rank k (ref. 1),

$$H_{\text{int}} = \sum_k T_c^{(k)} \cdot T_p^{(k)} \tag{6}$$

$T_c^{(k)}$ operates only on the degrees of freedom of the core and $T_p^{(k)}$ only on the particle coordinates. The exact nature of the core states are not specifically given. This gives the model a general validity, and it can therefore be applied to situations where the particle to core coupling is no longer weak, and allows several single-particle orbits to be considered. The Hamiltonian of the system is given by

$$H = H_c + H_p + H_{int} \tag{7}$$

where:

H_c Hamiltonian of core

H_p Hamiltonian of particle moving in field of core

H_{int} core to particle interaction

The basic set of states used for the calculation will be eigenfunctions of $H_c + H_p$ and are written as $|J_c j_p, IM\rangle$ where J_c and j_p are the spin of the core and particle, respectively, I is the total angular momentum of the coupled core and particle, and M is the z projection of I.

Only two core states will be considered. These are the O^+ ground state and the 2^+ state at 1.348 MeV in ^{64}Ni. The single-particle orbitals that are used are the $2p_{3/2}$, $2p_{1/2}$, and $1f_{5/2}$. The ^{64}Ni core closes the $1f_{7/2}$ proton orbital with 28 protons, so the three orbitals used are the only odd parity orbitals of low enough energy. Since the basis states used in the calculation, in general, will not be eigenfunctions of H_{int}, the eigenfunctions of H will be linear combinations of the basis states and will be obtained by diagonalizing the H matrix.

The form used for the interaction potential is that used by Thankappan and True (ref. 8)

$$H_{int} = -\xi(\vec{J}_c \cdot \vec{j}_p) - \eta(\vec{Q}_c \cdot \vec{Q}_p) \tag{8}$$

where J_c and j_p are the total angular momentum operator for the core and the particle, respectively; ξ and η are strength parameters; and Q_c and Q_p are the mass quadrupole-moment operators of the core and particles, respectively, where

$$\left(Q_c\right)_\mu = \sum_j r_j^2 Y_{2\mu}(\theta_i, \varphi_i) \tag{9}$$

$$\left(Q_p\right)_\mu = r_p^2 Y_{2\mu}(\theta_p, \varphi_p) \tag{10}$$

The matrix element of H between two basis states is then given by

$$\langle J_c' j_p', IM | H | J_c j_p, IM \rangle = \langle J_c' j_p', IM | H_c + H_p - \xi(\vec{J}_c \cdot \vec{j}_p) - \eta(\vec{Q}_c \cdot \vec{Q}_p) | J_c j_p, IM \rangle \quad (11)$$

$$\langle J_c' j_p', IM | H | J_c j_p, IM \rangle = \delta_{J_c' J_c} \delta_{j_p' j_p} \Big\{ E_{J_c} + E_{j_p} + \xi W(1 j_p J_c I; j_p J_c)$$

$$\left[J_c(J_c + 1)(2J_c + 1) j_p(j_p + 1)(2j_p + 1) \right]^{1/2} \Big\}$$

$$- \eta W(2 j_p' J_c I; j_p J_c') \langle J_c' || \vec{Q}_c || J_c \rangle \langle j_p' || \vec{Q}_p || j_p \rangle \quad (12)$$

where E_{J_c} and E_{j_p} are the energy eigenvalues of H_c and H_p, respectively. The reduced matrix elements used are the ones defined in Messiah (ref. 20). The particle reduced matrix elements can be calculated and are

$$\langle j_p' || \vec{Q}_p || j_p \rangle = \frac{(-1)^{(1/2) - j_p'}}{2} \langle j_p' | r_p^2 | j_p \rangle \left[\frac{(2j_p + 1)(2j_p' + 1)}{4\pi} \right]^{1/2} \left[1 + (-1)^{l + l'} \right] C\left(j_p j_p' 2; \frac{1}{2} - \frac{1}{2} 0 \right) \quad (13)$$

The W coefficients and Clebsh-Gordon coefficients were obtained from an existing computer program (ref. 21). The radial integral was evaluated using harmonic oscillator wave functions. The value of the parameter ν, for the harmonic oscillator wavefunction used was

$$\nu = \frac{41m}{\hbar^2 A^{1/3}} = 0.245 \text{ F}^{-2} \quad (14)$$

Since the model doesn't specify the exact nature of the core states, it is not possible to calculate the reduced matrix elements for the $\langle J_c' || \vec{Q}_c || J_c \rangle$, so these quantities are treated as parameters. For the ^{65}Cu calculation only the ground state and the first excited 2^+ core states were considered. It was assumed that the presence of the extra core proton did not alter the core states and they were taken as the same states that exist in ^{64}Ni. The three single-particle states used were the $2p_{1/2}$, $2p_{3/2}$, and $1f_{5/2}$ orbitals. The energy spacing between the $p_{3/2} - p_{1/2}$ orbitals and $p_{3/2} - f_{5/2}$ orbitals were taken from the ^{63}Cu calculation (ref. 8) and adjusted slightly for better agreement with the data. With the single-particle energies fixed, the three remaining adjustable parameters of the model are

(1) ξ is the dipole-dipole strength (15)

(2) $\chi_1 = \eta\langle 0||\vec{Q}_c||2\rangle$ (16)

(3) $\chi_2 = \eta\langle 2||\vec{Q}_c||2\rangle$ (17)

The electric quadrupole moment operator can be written as

$$\vec{Q}_e = \left(\frac{16\pi}{5}\right)^{1/2}\left[e_c\left(\vec{Q}_c\right)_0 + e\left(\vec{Q}_p\right)_0\right] \tag{18}$$

where

$$e_c = \frac{\sum e_j r_j^2 Y_{20}(\theta_i\varphi_i)}{\sum r_j^2 Y_{20}(\theta_i\varphi_i)} \tag{19}$$

is defined as an effective charge for the core. The reduced E2 transition probability from an initial state of spin I_1 to a final state of spin I_2 is given by

$$B(E2, I_1 \rightarrow I_2) = \frac{5}{16\pi(2I_1 + 1)}\left|\langle I_2||\vec{Q}_e||I_1\rangle\right| \tag{20}$$

Since it has been assumed that the core states of the ^{65}Cu nucleus are identical to the states of ^{64}Ni, it is possible to calculate

$$\langle 0||e_c\vec{Q}_c||2\rangle = [5B(E2)\downarrow]^{1/2}$$

where the $B(E2)\downarrow$ value is that of the first 2^+ state of the ^{64}Ni nucleus. The positive square root is taken to obtain agreement with the experimental data. So now for a given χ_1 and χ_2, the reduced matrix element $\langle 2||\vec{Q}_c||2\rangle$ is determined by

$$\langle 2||\vec{Q}_c||2\rangle = \frac{\chi_2}{\chi_1}\langle 0||\vec{Q}_c||2\rangle \tag{21}$$

Once ξ, χ_1, and χ_2 have been determined, the B(E2) values can be calculated providing e_c can be considered as a constant which is independent of the core states.

RESULTS OF CALCULATIONS AND COMPARISON TO EXPERIMENTAL DATA

The Hamiltonians for the coupled spins were diagonalized and the energy eigenvalues and eigenfunctions obtained. A parameter search was not done as in the calculation of Larner (ref. 22), but a limited result of a gridded parameter study is shown in figures 7, 8, and 9. Also shown in the figures is R, the ratio of the calculated B(E2) to those experimentally measured for the ^{64}Ni core (ref. 3). The energy of the lowest $3/2^-$ level has been set equal to zero in these figures. The final values of the parameters chosen were $\xi = 0.20$, $\chi_1 = 0.40$, and $\chi_2 = 0.35$. In figure 10 the resulting energy levels are shown and compared to the experimental data. To obtain better agreement with the experimental data, it was necessary to reduce the $p_{1/2} - p_{3/2}$ energy spacing from 1.30 MeV (ref. 8) to a new value of 1.20 MeV. The final values used for the calculation are shown in figure 10. The agreement is very good for the low-lying states, although the $3/2^-$ state at 1.725 MeV is not reproduced by the calculation.

The calculated ratios of B(E2) are compared to the experimental data in table IV. Since no octupole-octupole terms were included in the interaction potential, E3 reduced transition probabilities could not be calculated. The large errors in the experimental values of R make it difficult to compare the ratios; although for the three lowest states, agreement exists within the experimental error.

In table V the components of the wavefunctions for the calculated energy levels are listed. The square of the amplitudes of the $|0, j_p\rangle$ component of the eigenfunctions gives the percentages of the single-particle admixtures in a level and should be equal to the spectroscopic factors measured in proton stripping reactions. Listed in table V are the spectroscopic factors measured by Blair (ref. 6) in the ^{64}Ni(^{3}He, d) ^{65}Cu reaction. The calculated spectroscopic factors agree quite well with Blair's experimental results. The wavefunctions show considerable configuration mixing and explain the large collective and single-particle nature of some of the ^{65}Cu states.

CONCLUSIONS

The experimental data for the scattering of 42-MeV alpha particles from ^{65}Cu cannot be explained on the basis of the zero-strength particle-core coupling model. The number of observed states and their centroid energies do not agree with its predictions. There are seven states observed experimentally with an $l = 2$ angular momentum transfer, and eight states with an $l = 3$ angular momentum transfer. The $l = 2$ state at 2.858 MeV may result from coupling to a two-phonon state of the core. Considering all the $l = 2$ and $l = 3$ transition strength measured experimentally in ^{65}Cu, the total core transition strength of the first 2^+ and 3^- states is not found. The extended particle-core calculation has shown that the coupling is not weak and considerable con-

figuration mixing of the low-lying levels results. The extended particle-core model gives a good description of the energy levels for the low-lying states and predicts values of the single-particle strengths which are in fair agreement with the stripping data. The configuration mixing explains how the low-lying levels of ^{65}Cu can have large single-particle transition strengths and show strong collective behavior.

Lewis Research Center,
National Aeronautics and Space Administration,
Cleveland, Ohio, May 11, 1973,
503-10.

APPENDIX - SYMBOLS

A	nuclear mass number
a_i	diffuseness of imaginary term of nuclear optical potential
a_o	diffuseness of real term of nuclear optical potential
$B(E\ell)\uparrow$	reduced transition probability for transition from ground state to excited state by means of electric 2^ℓ-pole radiation
C^2S	spectroscopic strengths
e	electronic charge
e_c	effective charge of core
$f_{5/2}$	classification of nuclear state according to nuclear shell model
H	Hamiltonian of system of particles and core
H_c	Hamiltonian of core
H_{int}	Hamiltonian for core to particle interaction
H_p	Hamiltonian of particle moving in field of core
$\hbar^2$	Plank's constant squared
I	total angular momentum of coupled core and particle
J	total spin of system
J_c	spin of collective excitation of core
J_i	ground state spin of odd nucleus
J_f	excited state spin of odd nucleus
j_p	spin of extra core particles
ℓ	angular momentum transfer involved in reaction
M	z projection of I
m	particle mass
$p_{1/2}, p_{3/2}$	classification of nuclear states according to nuclear shell model
Q_e	electric quadrupole moment operator
$(Q_c)_\mu$	μ-component of core mass quadrupole moment operator
$(Q_p)_\mu$	μ-component of particle mass quadrupole moment operator

R	ratio of ^{65}Cu reduced transition probability to reduced transition probability of ^{64}Ni
R_o	nuclear radius constant
r_i	radius of imaginary term of nuclear optical potential
r_j	radius in core quadrupole moment operator
r_o	radius of real term of nuclear optical potential
r_p	radius in particle quadrupole moment operator
$T_c^{(k)}$	k^{th} component of operator that operates only on degrees of freedom of core
$T_p^{(k)}$	k^{th} component of operator that operates only on degrees of freedon of particle
$U(r)$	scattering potential
V	strength of real term of nuclear optical potential
V_c	Coulomb potential
W	strength of imaginary term of nuclear optical potential
$Y_{2\mu}(\theta_i, \varphi_i)$	spherical harmonic of order $2, \mu$
Z	nuclear charge
$\beta_l(^AX)$	deformation parameter of even A nucleus X
$\beta_l(\text{core})$	deformation parameter of even core
$\beta_l'(J_f)$	partial deformation parameter for final state of nucleus
η	strength of quadrupole term in interaction Hamiltonian
ν	harmonic oscillator parameter
ξ	strength of angular momentum term in interaction Hamiltonian
π	parity of nuclear state
χ_1	strength of nondiagonal quadrupole term of interaction Hamiltonian
χ_2	strength of diagonal quadrupole term of interaction Hamiltonian
$\left(\frac{d\sigma}{d\Omega}\right)_{J_f}^{exp}$	experimental differential cross section for spin state J_f
$\left(\frac{d\sigma}{d\Omega}\right)_{DWBA}$	differential cross section calculated by distorted wave Born approximation

REFERENCES

1. de-Shalit, A.: Core Excitations in Nondeformed, Odd-A, Nuclei. Phys. Rev., vol. 122, no. 5, June 1, 1961, pp. 1530-1536.

2. Harvey, B. G.; Meriwether, J. R.; Bussière, A.; and Horen, D. J.: Excitation of Collective Levels in Cu^{63} by 50 MeV α Scattering. Nucl. Phys., vol. 70, 1965, pp. 305-312.

3. McCarthy, A. L.; and Crawley, G. M.: Inelastic Proton Scattering on the Isotopes Ni^{62}, Ni^{64}, Cu^{63}, and Cu^{65} at 17.5 MeV. Phys. Rev., vol. 150, no. 3, Oct. 21, 1966, pp. 935-940.

4. Kumabe, Isao; Matoba, Masaru; and Takasaki, Eiichi: Inelastic Alpha-Particle Scattering on Copper 65 at 29 MeV. J. Phys. Soc. Japan, vol. 25, no. 2, Aug. 1968, pp. 301-306.

5. Bruge, G.; Faivre, J. C.; Barloutaud, M.; Faraggi, H.; and Saudinos, J.: Diffusion Inelastique De Particules α par Ni^{62}, Cu^{63}, Ni^{64}, Cu^{65} et Interaction Coeur-Particule. Phys. Letters, vol. 7, no. 3, Nov. 15, 1963, pp. 203-206.

6. Blair, A. G.: $Ni^{62,64}(He^3, d)\ Cu^{63,65}$ Reaction. Phys. Rev., vol. 140, no. 3B, Nov. 8, 1965, pp. 648-654.

7. Bachner, D.; Bock, R.; Duhm, H. H.; Santo, R.; Stock, R.; and Hinds, S.: Study of ^{63}Cu and ^{65}Cu Levels By The (t, α) Reaction. Nucl. Phys., vol. A99, 1967, pp. 487-496.

8. Thankappan, V. K.; and True, William W.: Properties of the Low-Lying Cu^{63} Levels. Phys. Rev., vol. 137, no. 4B, Feb. 22, 1965, pp. 793-799.

9. Wong, S. S. M.: A Shell-Model Study of ^{65}Cu and ^{63}Cu. Nucl. Phys., vol. A159, 1970, pp. 235-248.

10. Baron, Norton; and Kaminski, Gerald A.: Manufacture of Lithium-Drifted Silicon Surface-Barrier Semiconductor Counters. NASA TN D-3554, 1966.

11. Leonard, Regis F.; Stewart, William M.; and Baron, Norton: Alpha-Gamma Angular Correlations in the Reaction Tin-120 (α, $\alpha' \gamma_{1.18\ MeV}$). NASA TN D-5569, 1969.

12. Kern, Jean: Computer Analysis of Nuclear Spectra and γ-Energy Standards. Nucl. Inst. Meth., vol. 79, 1970, pp. 233-239.

13. Smith, Margaret M.; and Giamati, Charles C.: Expanded Fortran IV Program for Elastic Scattering Analysis. NASA TN D-6000, 1970.

14. Nathan, O.; and Nilsson, S. G.: Collective Nuclear Motion and the Unified Model. Alpha-, Beta-, and Gamma-Ray Spectroscopy. Vol. 1. K. Siegbahn, ed., North-Holland Pub., 1965, pp. 601-700.

15. Nucl. Data, Sec. B, vol. 2, no. 6, Oct. 1968.

16. Broek, H. W.: Collective Excitations in $Ni^{58,60,62}$ and $Zn^{64,66,68}$. Phys. Rev., vol. 130, no. 5, June 1, 1963, pp. 1914-1925.

17. Meriwether, J. R.; Bussiere De Nercy, A.; Harvey, B. G.; and Horen, D. J.: Energy Variation of the Phase Rule in Alpha Particle Scattering. Phys. Letters, vol. 11, no. 4, Aug. 15, 1964, pp. 299-300.

18. Perey, F.; Silva, R. J.; and Satchler, G. R.: Excited-Core Model of Odd-A Nuclei and the $Cu^{63}(p, p')$ Reactions. Phys. Letters, vol. 4, no. 1, Mar. 1, 1963, pp. 25-27.

19. Stewart, William M.; Baron, Norton; and Leonard, Regis F.: Core Excitations in Silver, Indium, and Antimony Resulting From Inelastic Scattering of 42-MeV (6.7-PJ) Alpha Particles. NASA TN D-4222, 1967.

20. Messiah, Albert (G. M. Temmer, trans.): Quantum Mechanics. John Wiley & Sons, Inc., 1961.

21. Ford, William F.; and Braley, Richard C.: Fortran IV Subroutines for Coupling Coefficients and Matrix Elements in the Quantum Mechanical Theory of Angular Momentum. NASA TN D-6173, 1971.

22. Larner, D.: Intermediate Coupling in the N = 29 and Z = 29 Nuclei. Phys. Rev., vol. 2, no. 2C, Aug. 1970, pp. 522-530.

TABLE I. - CROSS SECTIONS

[Incident energy, E_α = 42.33 MeV]

Laboratory scattering angle, θ_{lab}, deg	Center of mass scattering angle, θ_{cm}, deg	$\frac{d\sigma}{d\Omega} \pm \Delta\frac{d\sigma}{d\Omega}$, mb/sr
^{65}Cu elastic scattering		
8.0	8.49	75 029±366
9.0	9.55	51 055±225
10.0	10.61	26 934±220
11.0	11.67	16 113±126
12.0	12.73	8 130±120
13.0	13.79	5 622±74
14.0	14.85	3 937±84
15.0	15.91	3 449±58
16.0	16.97	2 913±22
17.0	18.03	2 028±12
18.0	19.09	1 267±15
19.0	20.15	772±7
20.16	21.20	394±8
22.08	23.32	262±1
24.08	25.43	283±48
26.08	27.54	158.7±0.4
28.08	29.66	45.44±0.19
30.16	31.76	20.26±0.13
32.16	33.87	39.58±0.18
34.16	35.98	39.83±0.18
36.16	38.08	22.64±0.14
38.08	40.18	3.95±0.06
40.08	42.27	2.60±0.05
42.08	44.36	8.18±0.08
44.08	46.45	8.50±0.08
46.16	48.54	3.27±0.05
48.16	50.62	0.392±0.018
^{65}Cu alpha scattering, 0.771-MeV state		
10.0	10.61	9.30±0.48
12.0	12.74	3.04±0.18
14.0	14.86	1.18±0.06
20.16	21.22	1.72±0.04
22.08	23.34	0.944±0.028
24.08	25.45	0.238±0.014
26.08	27.56	0.552±0.021
28.08	29.67	0.879±0.027
30.16	31.78	0.539±0.021
32.16	33.89	0.138±0.011
34.16	35.99	0.0377±0.0056
36.16	38.09	0.184±0.012
38.08	40.19	0.282±0.015
40.08	42.29	0.220±0.013
42.08	44.38	0.0364±0.0054
44.08	46.48	0.0149±0.0035
46.16	48.56	0.0916±0.0087
48.16	50.65	0.0969±0.0090

Laboratory scattering angle, θ_{lab}, deg	Center of mass scattering angle, θ_{cm}, deg	$\frac{d\sigma}{d\Omega} \pm \Delta\frac{d\sigma}{d\Omega}$, mb/sr
^{65}Cu alpha scattering; 1.114-MeV state		
10.0	10.62	12.96±0.44
12.0	12.74	11.32±0.36
14.0	14.86	4.20±0.22
16.0	16.98	2.54±0.17
20.16	21.22	6.62±0.07
24.08	25.46	0.593±0.022
26.08	27.57	0.888±0.026
28.08	29.68	2.38±0.08
30.16	31.79	2.08±0.04
32.16	33.89	0.740±0.024
34.16	36.00	0.134±0.010
36.16	38.10	0.269±0.014
38.08	40.20	0.961±0.028
40.08	42.30	0.892±0.027
42.08	44.39	0.257±0.014
44.08	46.48	0.029±0.005
46.16	48.57	0.218±0.013
^{65}Cu alpha scattering; 1.482-MeV state		
10.0	10.62	16.22±0.54
12.0	12.74	11.56±0.36
14.0	14.87	4.01±0.21
16.0	16.99	1.14±0.12
18.16	19.11	4.60±0.06
20.16	21.26	7.55±0.47
22.08	23.34	3.81±0.06
24.08	25.46	0.478±0.020
26.08	27.58	0.976±0.028
28.08	29.69	2.58±0.05
30.16	31.80	2.24±0.04
32.16	33.90	0.707±0.024
34.16	36.01	0.130±0.010
36.16	38.12	0.356±0.017
38.08	40.22	0.972±0.028
40.08	42.31	0.902±0.027
42.08	44.40	0.276±0.015
44.08	46.50	0.0373±0.0056
46.16	48.58	0.242±0.014
48.16	50.68	0.482±0.020

TABLE I. - Continued. CROSS SECTIONS

[Incident energy, E_α = 42.33 MeV.]

Laboratory scattering angle, θ_{lab}, deg	Center of mass scattering angle, θ_{cm}, deg	$\frac{d\sigma}{d\Omega} \pm \Delta \frac{d\sigma}{d\Omega}$, mb/sr
^{65}Cu alpha scattering; 1.629-MeV state		
10.0	10.62	1.48±0.11
12.0	12.74	0.515±0.076
18.16	19.11	0.225±0.012
20.16	21.23	0.374±0.017
24.08	25.46	0.0613±0.0042
26.08	*27.58*	*0.117±0.010*
30.16	31.80	0.0456±0.0060
32.16	33.91	0.0342±0.0052
34.16	36.02	0.0376±0.0060
36.16	38.12	0.0336±0.0052
40.08	42.31	0.0494±0.0064
42.08	44.41	0.0232±0.0044
44.08	46.50	0.0058±0.0022
46.16	48.59	0.0092±0.0028
48.16	50.68	0.0234±0.0044
^{65}Cu alpha scattering; 1.725-MeV state		
10.0	10.62	0.629±0.084
12.0	12.75	0.996±0.106
18.16	19.11	0.242±0.011
20.16	21.23	0.371±0.017
24.08	25.46	*0.0308±0.005*
28.08	29.69	*0.0878±0.0084*
30.16	31.80	0.108±0.009
32.16	33.91	0.0400±0.0057
36.16	38.12	0.0041±0.0018
38.08	40.22	0.0214±0.0042
40.08	42.32	0.0247±0.0045
42.08	44.42	0.0248±0.0045
44.08	46.50	0.0058±0.0022
46.16	48.60	0.0250±0.0014
^{65}Cu alpha scattering; 2.098-MeV state		
10.0	10.62	3.199±0.224
12.0	12.75	1.922±0.148
14.0	14.87	0.206±0.048
16.0	16.99	0.367±0.064
18.16	19.12	0.675±0.023
20.16	21.24	0.434±0.018
22.08	23.36	0.0954±0.0088
24.08	25.48	0.122±0.010
26.08	27.59	0.226±0.014
28.08	29.70	0.262±0.015
34.16	36.02	0.0188±0.0039
36.16	38.13	0.0532±0.0066
38.08	40.23	0.0797±0.0080
40.08	42.33	0.0560±0.0068
42.08	44.42	0.0214±0.0042
44.08	46.52	0.0082±0.0026
46.16	48.61	0.0332±0.0052
48.16	50.69	0.0450±0.0061

Laboratory scattering angle, θ_{lab}, deg	Center of mass scattering angle, θ_{cm}, deg	$\frac{d\sigma}{d\Omega} \pm \Delta \frac{d\sigma}{d\Omega}$, mb/sr
^{65}Cu alpha scattering; 2.344-MeV state		
12.0	12.75	1.144±0.114
20.16	21.24	0.175±0.012
22.08	23.36	0.0372±0.0054
28.08	29.70	0.0649±0.0072
30.16	31.82	0.0504±0.0064
36.16	*38.14*	*0.0360±0.0054*
38.08	40.24	0.0164±0.0036
40.08	42.34	0.0288±0.0048
42.08	44.44	0.0174±0.0038
46.16	48.62	0.0182±0.0038
48.16	50.76	0.0183±0.0039
^{65}Cu alpha scattering; 2.530-MeV state		
10.0	10.63	7.862±0.432
12.0	12.76	8.352±0.293
14.0	14.88	7.185±0.286
16.0	17.00	3.035±0.186
18.16	19.12	0.829±0.026
20.16	21.24	0.892±0.026
22.08	23.36	2.758±0.047
24.08	25.48	2.974±0.049
26.08	27.60	1.048±0.029
30.16	31.82	0.724±0.024
32.16	33.93	1.294±0.032
36.16	38.14	0.526±0.020
38.08	40.24	0.0920±0.0086
40.08	42.34	0.226±0.014
42.08	44.44	0.497±0.020
44.08	46.53	0.412±0.018
46.16	48.62	0.128±0.010
48.16	50.71	0.0316±0.0051
^{65}Cu alpha scattering; 2.858-MeV state		
10.0	10.63	1.484±0.130
12.0	12.76	0.982±0.106
14.0	14.88	0.286±0.057
18.16	19.13	0.371±0.017
20.16	21.25	0.422±0.018
22.08	23.37	0.184±0.012
24.08	25.49	0.0420±0.0058
26.08	27.60	0.1069±0.0093
28.08	29.72	0.193±0.012
30.16	31.83	0.176±0.012
32.16	33.94	0.0774±0.0079
34.16	36.04	0.0670±0.0074
38.08	40.26	0.1010±0.0091
40.08	42.36	0.0898±0.0086
42.08	44.45	0.0809±0.0082
44.08	46.54	0.0282±0.0048
46.16	48.64	0.0299±0.0050
48.16	50.72	0.0433±0.0060

TABLE I. - Continued. CROSS SECTIONS

[Incident energy, E_α = 42.33 MeV.]

Laboratory scattering angle, θ_{lab}, deg	Center of mass scattering angle, θ_{cm}, deg	$\frac{d\sigma}{d\Omega} \pm \Delta \frac{d\sigma}{d\Omega}$, mb/sr
^{65}Cu alpha scattering; 2.980-MeV state		
10.0	10.63	1.472±0.073
12.0	12.76	1.689±0.082
14.0	14.88	1.345±0.073
16.0	17.01	0.183±0.027
18.16	19.13	0.137±0.006
20.16	21.25	0.174±0.007
22.08	23.37	0.458±0.011
24.08	25.49	0.514±0.012
26.08	27.60	0.194±0.008
28.08	29.72	0.0327±0.0030
32.16	33.94	0.185±0.008
34.16	36.04	0.214±0.008
38.08	40.26	0.038±0.003
40.08	42.36	0.034±0.003
42.08	44.45	0.080±0.005
44.08	46.54	0.074±0.004
^{65}Cu alpha scattering; 3.082-MeV state		
10.0	10.63	4.213±0.212
12.0	12.75	4.853±0.235
14.0	14.88	3.864±0.210
16.0	17.01	0.526±0.078
18.16	19.13	0.396±0.018
20.16	21.26	0.500±0.020
22.08	23.38	1.315±0.032
24.08	25.50	1.478±0.034
26.08	27.61	0.558±0.022
28.08	29.72	0.0941±0.0087
32.16	33.94	0.582±0.022
34.16	36.05	0.614±0.022
38.08	40.26	0.110±0.010
40.08	42.36	0.128±0.010
42.08	44.45	0.230±0.014
44.08	46.55	0.212±0.013
46.16	48.64	0.0664±0.0074
48.16	50.73	0.0466±0.0062
^{65}Cu alpha scattering; 3.310-MeV state		
10.0	10.64	4.399±0.220
12.0	12.76	4.977±0.238
14.0	14.89	3.474±0.199
16.0	17.02	2.013±0.151
18.16	19.14	0.426±0.018
20.16	21.26	0.739±0.024
22.08	22.38	1.394±0.034
24.08	25.50	1.314±0.032
26.08	27.62	0.610±0.022
28.08	29.73	0.304±0.016
34.16	36.06	0.584±0.022
36.16	38.16	0.351±0.016
40.08	42.37	0.181±0.012
42.08	44.46	0.308±0.016
44.08	46.56	0.243±0.014
46.16	48.65	0.108±0.010
48.16	50.74	0.113±0.010

Laboratory scattering angle, θ_{lab}, deg	Center of mass scattering angle, θ_{cm}, deg	$\frac{d\sigma}{d\Omega} \pm \Delta \frac{d\sigma}{d\Omega}$, mb/sr
^{65}Cu alpha scattering; 3.494-MeV state		
10.0	10.64	3.649±0.202
12.0	12.76	4.051±0.214
14.0	14.89	3.061±0.187
16.0	17.01	1.669±0.138
18.16	19.14	0.560±0.021
20.16	21.26	0.482±0.020
22.08	23.38	1.089±0.030
24.08	25.50	1.183±0.031
26.08	27.62	0.581±0.022
28.08	29.74	0.174±0.012
30.16	31.84	0.236±0.014
32.16	33.95	0.580±0.022
34.16	36.06	0.482±0.019
36.16	38.17	0.388±0.018
38.08	40.28	0.1116±0.0096
42.08	44.47	0.229±0.014
44.08	46.56	0.208±0.013
46.16	48.66	0.110±0.010
48.16	50.74	0.0416±0.0058
^{65}Cu alpha scattering; 3.709-MeV state		
10.0	10.64	0.912±0.102
12.0	12.77	1.186±0.116
14.0	14.90	0.891±0.101
16.0	17.02	0.892±0.101
18.16	19.14	0.278±0.014
20.16	21.26	0.370±0.017
22.08	23.38	0.476±0.020
24.08	25.50	0.358±0.017
26.08	27.62	0.262±0.014
28.08	29.73	0.199±0.012
30.16	31.85	0.112±0.010
32.16	33.96	0.148±0.012
34.16	36.08	0.140±0.010
36.16	38.18	0.115±0.010
40.08	42.38	0.0467±0.0038
42.08	44.48	0.0726±0.0077
44.08	46.58	0.0910±0.0086
46.16	48.66	0.0805±0.0082
48.16	50.75	0.0383±0.0056
^{65}Cu alpha scattering; 3.930-MeV state		
10.0	10.64	1.310±0.122
12.0	12.77	0.952±0.092
16.0	17.02	0.468±0.073
22.08	23.39	0.222±0.013
24.08	25.51	0.212±0.013
26.08	27.63	0.134±0.010
28.08	29.74	0.0551±0.0066
32.16	33.97	0.115±0.010
34.16	36.08	0.123±0.010
38.08	40.29	0.0328±0.0052
40.08	42.39	0.0444±0.0060
46.16	48.67	0.0481±0.0063
48.16	50.76	0.0249±0.0046

TABLE I. - Concluded. CROSS SECTIONS

[Incident energy, E_α = 42.33 MeV.]

Laboratory scattering angle, θ_{lab}, deg	Center of mass scattering angle, θ_{cm}, deg	$\frac{d\sigma}{d\Omega} \pm \Delta \frac{d\sigma}{d\Omega}$, mb/sr
^{65}Cu alpha scattering; 4.047-MeV state		
10.0	10.64	1.994±0.150
12.0	12.77	1.744±0.140
14.0	14.90	2.236±0.159
16.0	17.02	1.712±0.139
18.16	19.15	0.591±0.022
20.16	21.27	0.524±0.024
22.08	23.39	0.798±0.025
24.08	25.52	0.789±0.025
26.08	27.63	0.344±0.016
28.08	29.74	0.216±0.013
30.16	31.86	0.262±0.014
32.16	33.97	0.276±0.015
34.16	36.08	0.370±0.017
38.08	40.29	0.121±0.010
42.08	44.49	0.164±0.012
46.16	48.68	0.0863±0.0084
48.16	50.77	0.0325±0.0052
^{65}Cu alpha scattering; 4.180-MeV state		
10.0	10.64	1.480±0.130
12.0	12.77	0.398±0.067
16.0	17.02	0.206±0.048
18.16	19.15	0.184±0.012
20.16	21.28	0.217±0.013
22.08	23.40	0.0532±0.0065
24.08	25.52	0.0322±0.0016
26.08	27.64	0.0856±0.0083
30.16	31.86	0.0511±0.0064
32.16	33.98	0.0830±0.0082
34.16	36.08	0.0562±0.0068
38.08	40.30	0.0934±0.0088
42.08	44.50	0.0536±0.0066
46.16	48.68	0.0382±0.0056
48.16	50.77	0.0333±0.0052

TABLE II. - OPTICAL MODEL PARAMETERS

Real well depth, V, MeV	195.9
Real well radius, r_o, f	1.364
Real well diffuseness, a_o, f	0.586
Imaginary well depth, W, MeV	21.93
Imaginary well radius, r_i, f	1.505
Imaginary well diffuseness, a_i, f	0.627

TABLE III. - EXPERIMENTAL INFORMATION

Energy level, MeV (a)	Angular momentum transfer, l	Partial deformation parameter, $\beta'_l(J_f)$	Spin and parity, J^π	Deformation parameter of even core, β_l(core)	R_{ALPHA}[b]	R_{PROTON}[b, c]	R_{ALPHA}[b, d]
0.771	2	0.0578	$1/2^-$	0.183±0.016	0.836±0.226	1.00±0.17	0.925
1.114	↓	.0977	$5/2^-$	.178±0.014	.795±0.208	1.21±0.22	.99
1.482	↓	.108	$7/2^-$	.172±0.014	.730±0.202	.95±0.18	.90
1.629	↓	.0234	$(5/2)^-$	.042±0.004	.045±0.012	.20±0.05	.09
1.725	↓	.0222	$3/2^-$	.049±0.003	.060±0.015	---------	.22
2.098	2	.0365	$(5/2)^-$	.066±0.005	.105±0.021	---------	.28
2.344	---	------	-----	----------	----------	---------	-----
2.530	3	.0864	$(9/2)^+$	.122±0.011	.455±0.136	1.25±0.20	-----
2.858	2	.0267	-----	----------	----------	---------	-----
2.980	3	.0390	-----	----------	----------	---------	-----
3.082	3	.0666	-----	----------	----------	---------	-----
3.310	↓	.0683	$(5/2)^+$	.124±0.011	.467±0.014	1.30±0.30	-----
3.494	↓	.0624	-----	----------	----------	---------	-----
3.709	↓	.0335	-----	----------	----------	---------	-----
3.930	↓	.0331	-----	----------	----------	---------	-----
4.047	↓	.0496	-----	----------	----------	---------	-----
4.180	---	------	-----	----------	----------	---------	-----

[a] Error in energy levels is ±25 keV.

[b] $R = \frac{B(E\ell)\uparrow^{65}Cu}{B(E\ell)\uparrow^{64}Ni}$.

[c] Ref. 3.

[d] Ref. 4.

TABLE IV. - RATIOS OF B(E2)

Energy level, MeV	Spin and parity, J^π	Deformation parameter, β_2(core)	R^a	Deformation parameter, β_2(core)	R^a	Deformation parameter, β_2(core)	R^a	R^a (calculation)
		Alpha scattering		Proton scattering[b]		Alpha scattering[c]		
0.771	$1/2^-$	0.183±0.016	0.836±0.226	0.200±0.010	1.00±0.17	0.174	0.925	1.003
1.114	$5/2^-$	.178±0.014	.795±0.208	.220±0.014	1.21±0.22	.181	.99	.786
1.482	$7/2^-$	.172±0.014	.730±0.202	.195±0.014	.95±0.18	.173	.90	.928
1.629	$(5/2)^-$	.042±0.004	.045±0.012	.078±0.007	.20±0.05	.055	.09	.440
1.725	$3/2^-$	.049±0.003	.060±0.015	----------	---------	.084	.22	-----
2.098	$(5/2)^-$	.066±0.005	.105±0.021	----------	---------	.097	.28	.420

[a] $R = \frac{B(E\ell)\uparrow^{65}Cu}{B(E\ell)\uparrow^{64}Ni}$.

[b] Ref. 3.

[c] Ref. 4.

TABLE V. - EIGENFUNCTIONS

Energy level, MeV	Spin and parity, J^{π}	$\|0, p_{1/2}\rangle$	$\|0, p_{3/2}\rangle$	$\|0, f_{5/2}\rangle$	$\|2, p_{1/2}\rangle$	$\|2, p_{3/2}\rangle$	$\|2, f_{5/2}$	C^2S	
								Calculated	Reference 6[a]
0	$3/2^-$	------	0.9286	------	0.1810	-0.3070	0.1034	0.86	0.79 $p_{3/2}$
.776	$1/2^-$	0.8809	------	------	------	-.4116	-.2334	.79	.75 $p_{1/2}$
1.143	$5/2^-$	------	------	0.7224	-.1044	-.6422	-.2343	.52	.26 $f_{5/2}$
1.451	$7/2^-$	------	------	------	------	.9869	.1612	----	.054
1.565	$5/2^-$	------	------	.5234	-.4243	.7194	-.1686	.27	.57 $f_{5/2}$
2.133	$3/2^-$	------	.1612	------	.5821	.7855	-.1345	----	.073 $f_{5/2}$

[a] $^{64}Ni(^3He, d)^{65}Cu$.

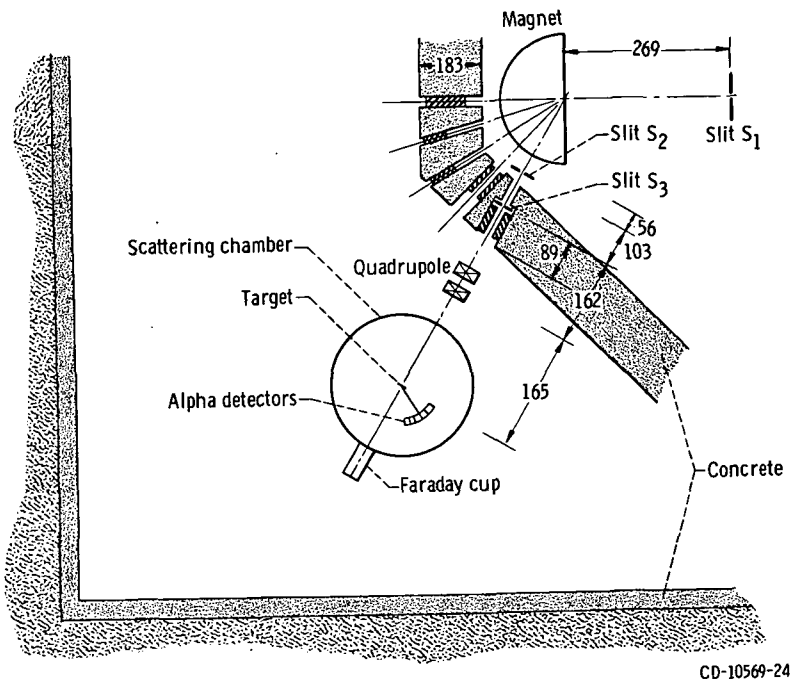

Figure 1. - Scattering system. (All dimensions are in cm.)

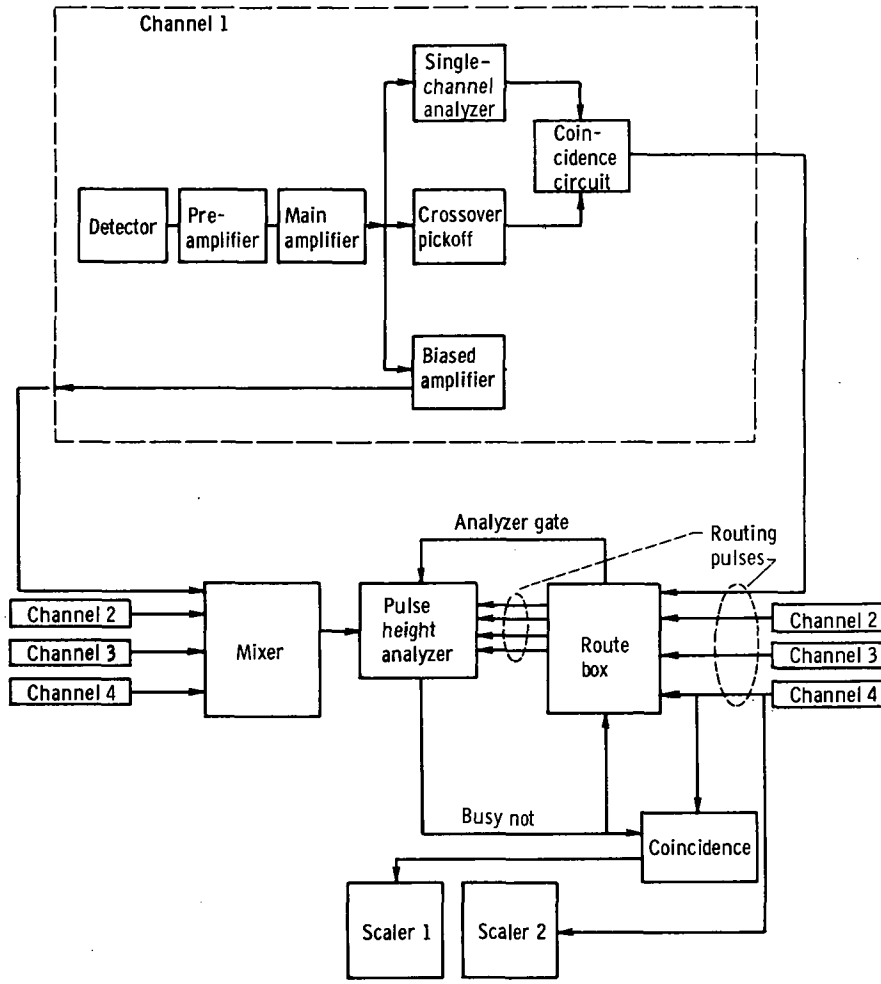

Figure 2. - Block diagram of electronics. (Channel 1 is shown in detail and is representative of channels 2, 3, and 4.)

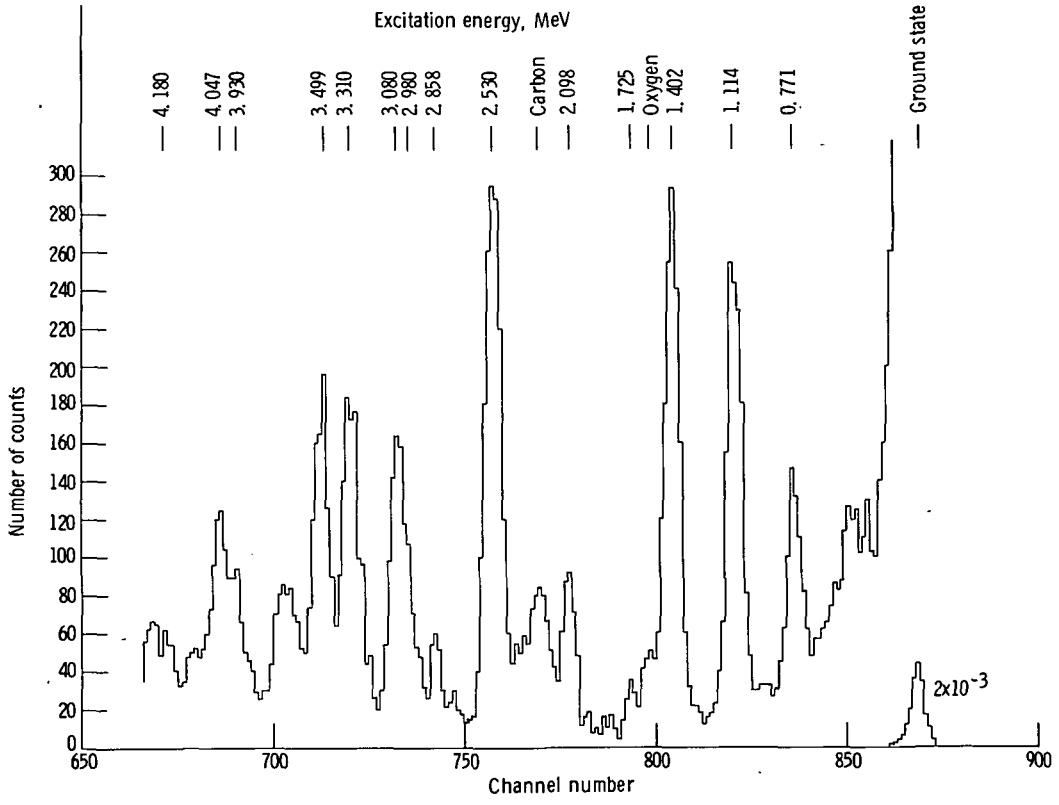

Figure 3. - Energy spectrum $^{65}Cu(\alpha,\alpha')$; laboratory scattering angle $\theta_{lab} = 26.0^{o}$.

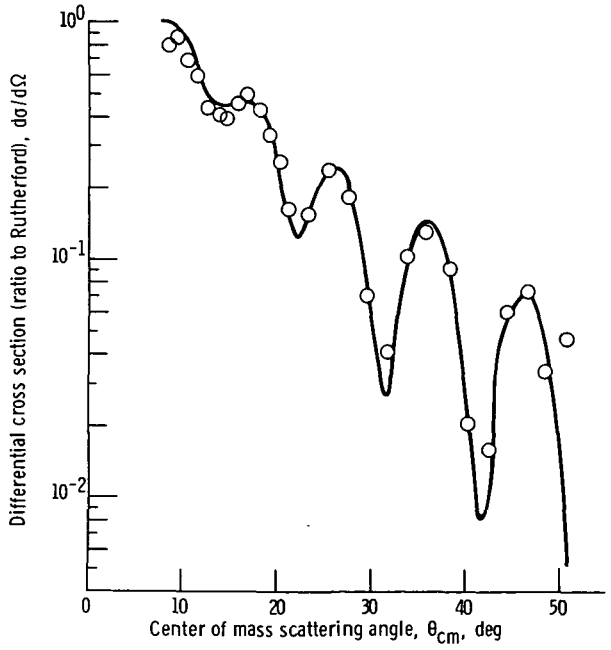

Figure 4. - ^{65}Cu elastic alpha scattering incident energy $E_{\alpha} = 42.33$ MeV. Real well depth V = 195.9 MeV; real well radius $r_0 = 1.364$ f; real well diffuseness $a_0 = 0.586$ f; imaginary well depth W = 21.93 MeV; imaginary well radius $r_i = 1.505$ f; imaginary well diffuseness $a_i = 0.627$ f.

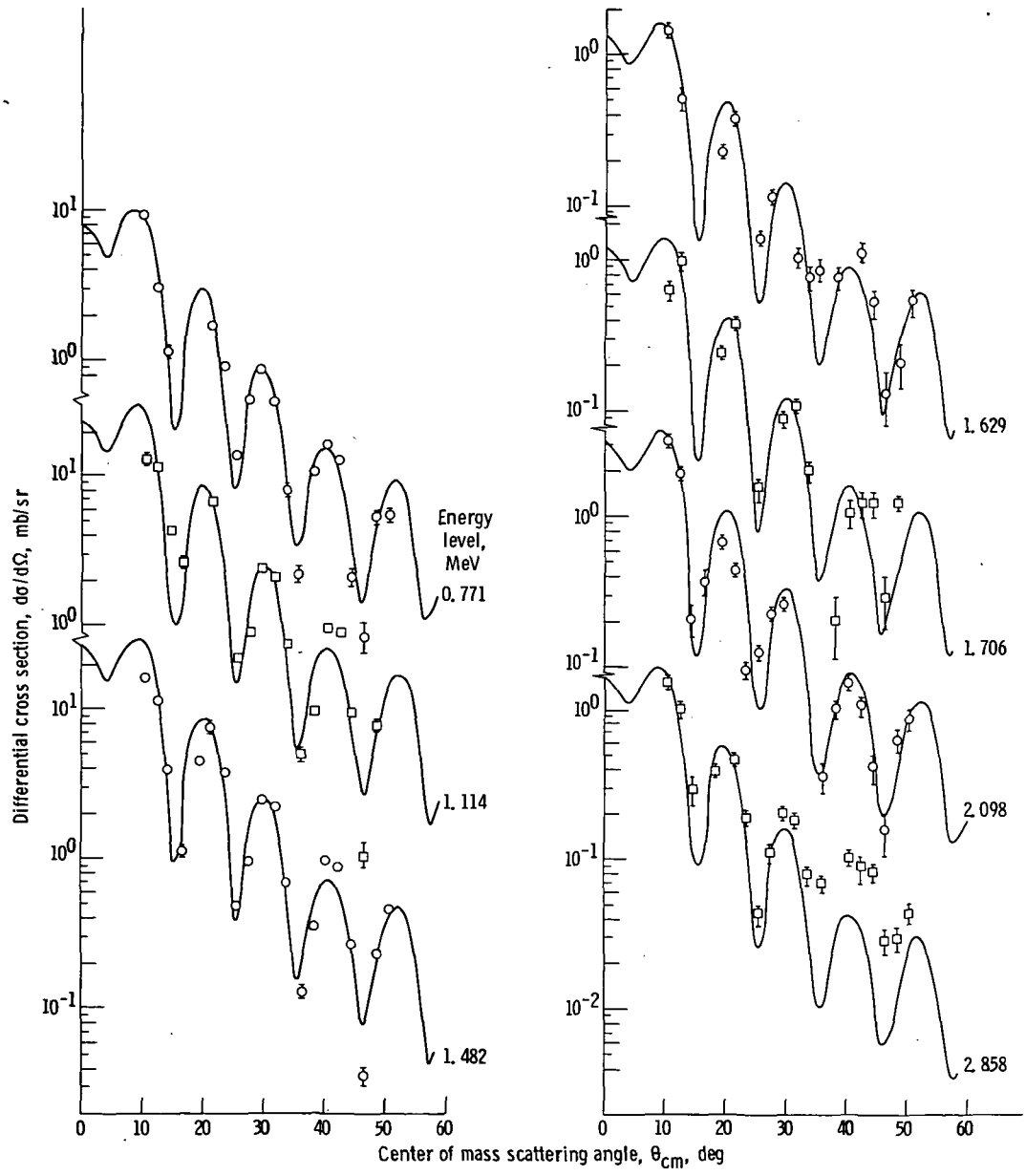

Figure 5. - $l = 2$ angular distributions.

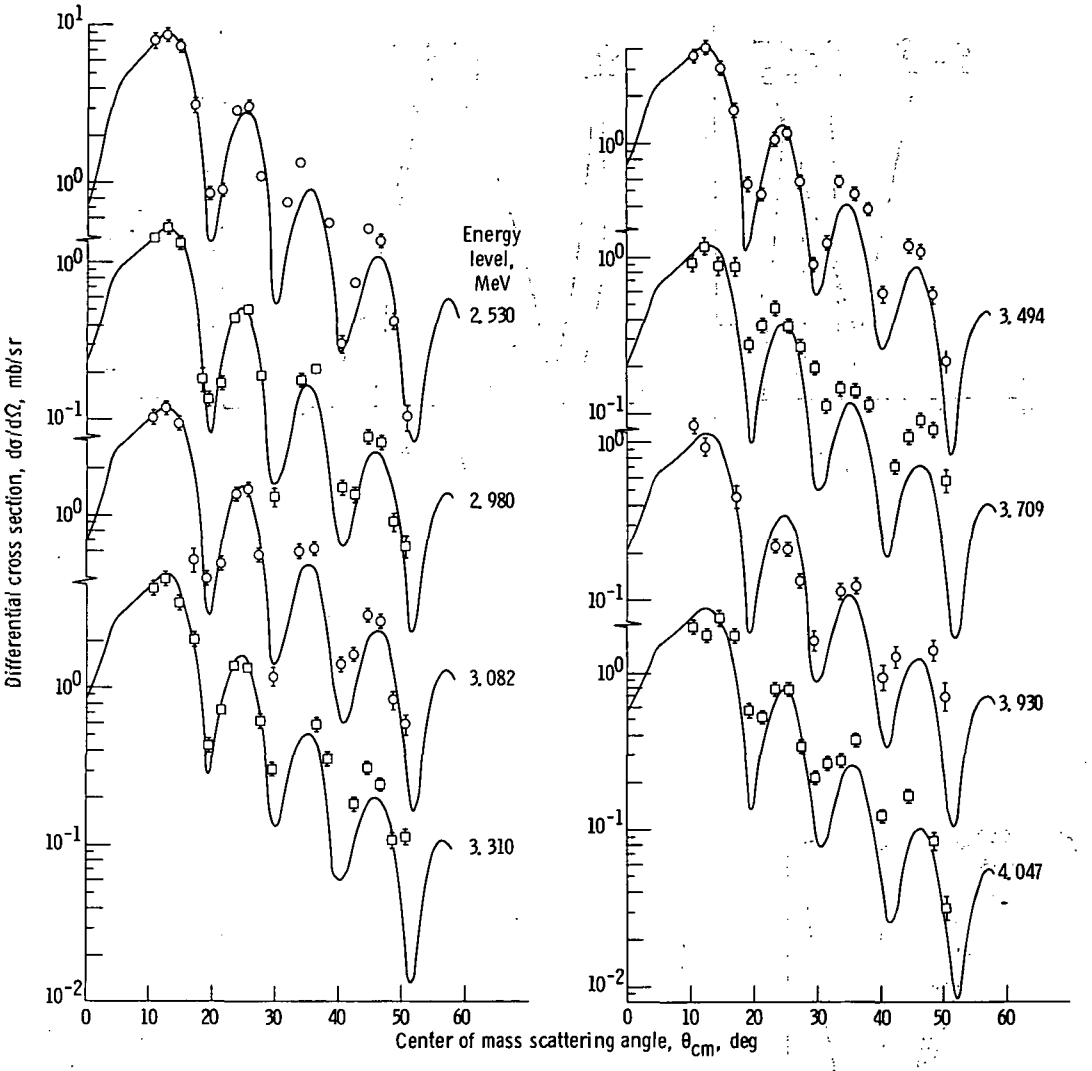

Figure 6. - l = 3 angular distributions.

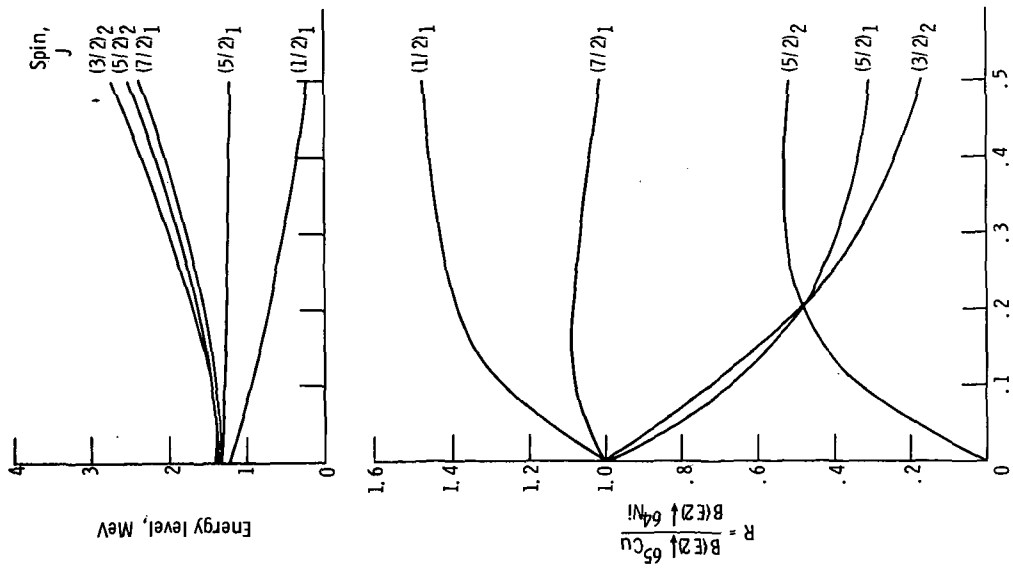

Figure 7. - Gridded parameter search on χ_1; $\xi = \chi_2 = 0$.

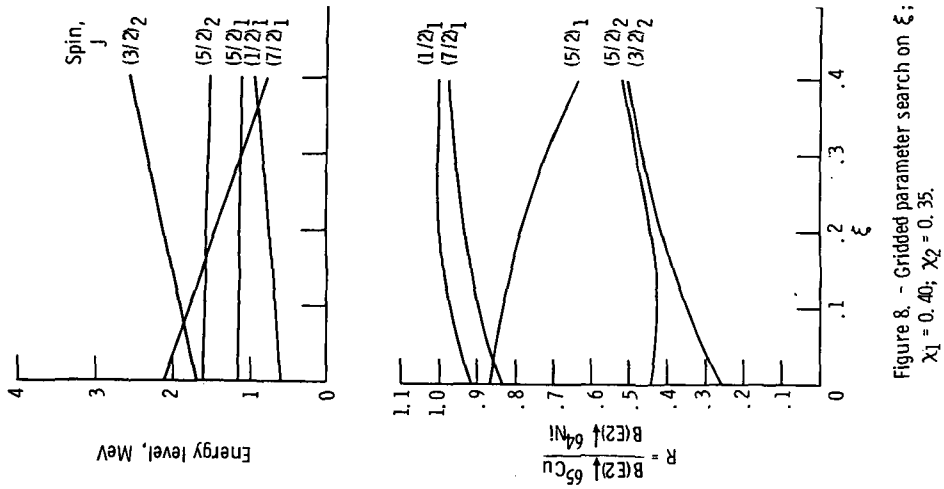

Figure 8. - Gridded parameter search on ξ; $\chi_1 = 0.40$; $\chi_2 = 0.35$.

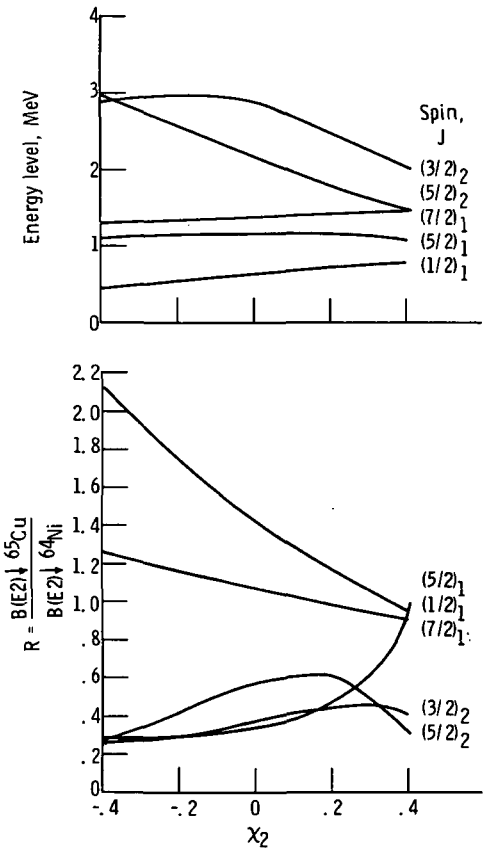

Figure 9. - Gridded parameter search on χ_2; $\xi = 0.20$; $\chi_1 = 0.40$.

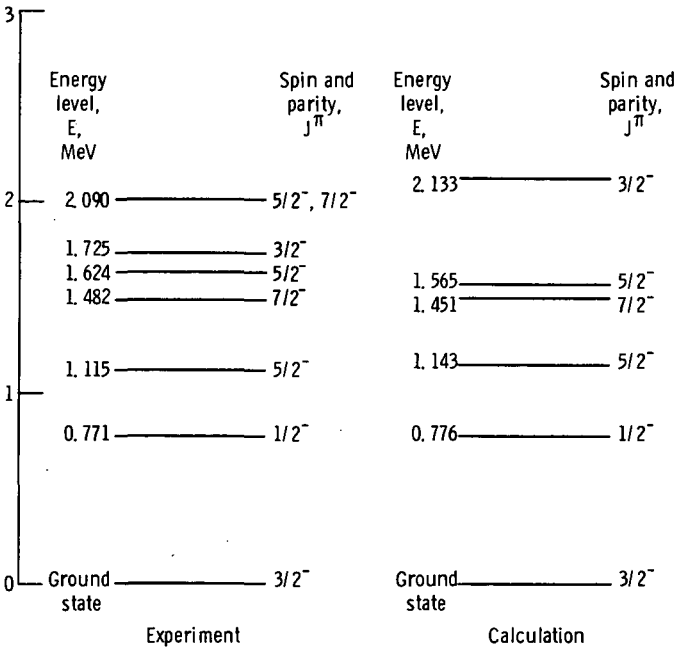

Figure 10. - Comparison of experimental and calculated energy level for ^{65}Cu. Calculation parameters: $p_{3/2} - p_{1/2} = 1.20$ MeV; $\xi = 0.20$; $p_{3/2} - f_{5/2} = 1.40$ MeV; $\chi_1 = 0.40$; $\chi_2 = 0.35$.

NATIONAL AERONAUTICS AND SPACE ADMINISTRATION
WASHINGTON, D.C. 20546

OFFICIAL BUSINESS
PENALTY FOR PRIVATE USE $300

SPECIAL FOURTH-CLASS RATE BOOK

POSTAGE AND FEES PAID
NATIONAL AERONAUTICS AND SPACE ADMINISTRATION
451

U.S.MAIL

POSTMASTER: If Undeliverable (Section 158 Postal Manual) Do Not Return

"The aeronautical and space activities of the United States shall be conducted so as to contribute . . . to the expansion of human knowledge of phenomena in the atmosphere and space. The Administration shall provide for the widest practicable and appropriate dissemination of information concerning its activities and the results thereof."

—NATIONAL AERONAUTICS AND SPACE ACT OF 1958

NASA SCIENTIFIC AND TECHNICAL PUBLICATIONS

TECHNICAL REPORTS: Scientific and technical information considered important, complete, and a lasting contribution to existing knowledge.

TECHNICAL NOTES: Information less broad in scope but nevertheless of importance as a contribution to existing knowledge.

TECHNICAL MEMORANDUMS: Information receiving limited distribution because of preliminary data, security classification, or other reasons. Also includes conference proceedings with either limited or unlimited distribution.

CONTRACTOR REPORTS: Scientific and technical information generated under a NASA contract or grant and considered an important contribution to existing knowledge.

TECHNICAL TRANSLATIONS: Information published in a foreign language considered to merit NASA distribution in English.

SPECIAL PUBLICATIONS: Information derived from or of value to NASA activities. Publications include final reports of major projects, monographs, data compilations, handbooks, sourcebooks, and special bibliographies.

TECHNOLOGY UTILIZATION PUBLICATIONS: Information on technology used by NASA that may be of particular interest in commercial and other non-aerospace applications. Publications include Tech Briefs, Technology Utilization Reports and Technology Surveys.

Details on the availability of these publications may be obtained from:

SCIENTIFIC AND TECHNICAL INFORMATION OFFICE

NATIONAL AERONAUTICS AND SPACE ADMINISTRATION

Washington, D.C. 20546